Journal of Magnetic Resonance 198 (2009) 228–235

Contents lists available at ScienceDirect

Journal of Magnetic Resonance

journal homepage: www.elsevier.com/locate/jmr

# Practical comparison of sensitivity and resolution between STMAS and MQMAS for $^{27}$Al

Takafumi Takahashi [a,*], Koji Kanehashi [a], Yuichi Shimoikeda [b], Takahiro Nemoto [b], Koji Saito [c]

[a] Advanced Technology Laboratories, Nippon Steel Corporation, 20-1 Shintomi, Futtsu, Chiba 293-8511, Japan
[b] JEOL Ltd., 3-1-2 Musashino, Akishima, Tokyo 196-8558, Japan
[c] Environment & Process Technology Center, Nippon Steel Corporation, 20-1 Shintomi, Futtsu, Chiba 293-8511, Japan

ARTICLE INFO

*Article history:*
Received 14 October 2008
Revised 27 February 2009
Available online 9 March 2009

*Keywords:*
STMAS
MQMAS
Resolution
Sensitivity
Kaolin
Glass
Quadrupolar
$^{27}$Al

ABSTRACT

An experimental comparison of sensitivity and resolution of satellite transition (ST) MAS and multiple quantum (MQ) MAS was performed for $^{27}$Al ($I = 5/2$) using several pulse sequences with a *z*-filter and SPAM, and two inorganic samples of kaolin ($Al_2Si_2O_5(OH)_4$) and glass ($43.1CaO–12.5Al_2O_3–44.4SiO_2$). Six pulse sequences of STMAS (double-quantum filter-soft pulse added mixing = DQF-SPAM, double-quantum filter = DQF, double-quantum = DQ) and MQMAS (3QMAS-*z*-filter = 3Qz, 3QMAS-SPAM = 3Q-SPAM, 5QMAS-*z*-filter = 5Qz) are employed. All experiments have been conducted utilizing a static field of 16.4 T (700 MHz for $^1$H) and a rotor spinning frequency of 20 kHz. Dependence of S/N ratios as a function of radio frequency (r.f.) field strengths indicates that strong r.f. fields are essential to obtain a better S/N ratio in all experiments. High sensitivity is obtained in the following order: DQF-SPAM, DQF, DQ, 3QSPAM, and 3Qz, although the degree of sensitivity enhancement given by STMAS for glass is slightly smaller than that for kaolin. This might be due to the different excitation and conversion efficiencies of ST and MQ coherences as a function $C_q$ values because quadrupolar interaction of the glass are widely distributed, or to motional broadening caused by framework flexibility in the structure of glass. With respect to resolution, the full widths at half maximum (FWHM) of $F_1$ projections of DQF-STMAS and 3QMAS spectra for kaolin are found to be comparable, which agrees with a simulated result reported in a literature. For glass, the STMAS possess slightly wider line widths than 3QMAS. However, because such a difference in line widths of STMAS and 3QMAS spectra is substantially small, we have concluded that STMAS and 3QMAS have comparable resolution for crystalline and non-crystalline materials.

© 2009 Elsevier Inc. All rights reserved.

## 1. Introduction

Solid state NMR for quadrupolar nuclei has been recognized as a very powerful analytical technique, but needs special care to obtain their high-resolution spectra. Because quadrupolar nuclei have an asymmetric distribution of nuclear charge, quadrupolar interaction occurs between the nuclear charge and the electric field gradient provided by the surrounding electrons [1]. The interaction can be treated as perturbation for Zeeman splitting that gives a set of equally-spaced energy levels as a result of interaction between magnetic moment of nuclear spin and a static magnetic field.

When quadrupolar interaction is much smaller than Zeeman interaction, satellite transitions (STs) mainly perturbed by first-order quadrupolar interaction are observed on an NMR spectrum in a manner symmetrically shifted from central transition (CT) [2]. By contrast, when quadrupolor interaction is sufficiently large as in most experiments for quadrupolar nuclei, STs perturbed by the first- and second-order quadrupolar interactions are asymmetrically observed around CT [3].

Multiple quantum (MQ) MAS NMR proposed by Frydman and Harwood [4] averages out second-order quadrupolar interaction utilizing the correlation of MQ and CT. One of the weak points of MQMAS is low sensitivity, which is due to low efficiency in excitation and conversion of MQ coherence. Therefore, application of MQMAS is limited to quadrupolar nuclei contained as abundant spins or those with isotopic labeling. As an alternative to MQMAS, Gan [5] proposed STMAS NMR where the correlation of ST and CT coherences are observed under rotor-synchronized condition. STMAS is similar to MQMAS in several ways, but superior to that in sensitivity, which is derived from the fact that single-quantum ST is more efficiently generated than MQ. Enhancement of sensitivity by STMAS at finite spinning frequencies has been evidenced in some simulative [6] and experimental [6–9] studies. The use of STMAS NMR not only cuts off the scan time needed in the conventional MQMAS experiments, but also provides a high-resolution spectrum of rare spins.

STMAS has additional advantages compared to MQMAS such as an improvement in quantification [6], and a wider spectral width

* Corresponding author. Fax: +81 439 87 7315.
*E-mail address:* takahashi.takafumi@nsc.co.jp (T. Takahashi).

1090-7807/$ - see front matter © 2009 Elsevier Inc. All rights reserved.
doi:10.1016/j.jmr.2009.02.015

in $F_1$ (isotropic) dimension as far as two rotor-synchronized experiments are compared [10].

On the other hand, STMAS requires more strict experimental conditions than MQMAS to obtain a reliable spectrum; miss setting of magic angle must be suppressed to be less than 0.002° [11], and the spectral width in $F_1$ (isotropic) dimension must be equal to the spinning frequency, which means that the FID sampling is performed at an integral number of rotor periods (=rotor-synchronization). If either of the two conditions is not satisfied, the STMAS spectrum should be splitting or broad because of the reintroduction of first-order quadrupolar interaction.

Several techniques are proposed to acquire a practically useful STMAS spectrum without undesired signals. For instance, in a STMAS spectrum obtained with a simple two-pulse sequence, the undesired signals such as CT–CT autocorrelation ridges and the resonances arising from outer $ST_n\{(\pm m, \pm(m-1))$ for $m > 3/2\}$ – CT correlation appear. These signals containing no useful structural information only make the interpretation complicated. Implementation of double-quantum filter (DQF) or double-quantum (DQ) techniques into STMAS is a robust way to remove the undesired signals [12]. Furthermore, the other scheme can be implemented into a basic STMAS pulse sequence to improve the sensitivity of STMAS. The soft pulse added mixing (SPAM) [13,14] combined with a DQF enhances the sensitivity by a factor of 2 compared to the original one [15].

Although the signal advantage of STMAS with respect to MQMAS has been reported by a few numerical calculations and some experiments, practical effects of STMAS on sensitivity and resolution have not been sufficiently understood. Therefore, the purpose of this study is to investigate the practical effects of STMAS on sensitivity and resolution in $^{27}Al$ ($I = 5/2$) measurements. Kaolin (clay mineral) and glass, which are different in quadrupolar interactions and in crystallinity, have been used as models of industrially useful inorganic compounds. In the comparison of sensitivity and resolution, changes of signal to noise (S/N) ratios and line widths depending on r.f. field strengths has been examined using several sequences of STMAS and MQMAS. This study covers the comparison of only the experiments utilizing a *z*-filter and echo/antiecho SPAM, although the phase-modulated experiments such as whole-echo acquisition have been recognized to be common for getting higher signal to noise ratios. Based on the comparison, the advantage of STMAS over MQMAS in the structural analysis of practical materials has been discussed.

## 2. Experimental

### 2.1. Preparation

Two inorganic materials of kaolin ($Al_2Si_2O_5(OH)_4$, quadrupolar products $P_Q = 3.6$ MHz) [16] and glass ($43.1CaO–12.5Al_2O_3–44.4SiO_2$, $P_Q = 7.2$ MHz) [17] were chosen as models of useful inorganic compounds. Kaolin was purchased from Aldrich Chemical Company, Inc., while the glass was synthesized from a reagent-grade, well dried starting materials to have a composition of 43.1 mol% CaO, 12.5 mol% $Al_2O_3$, and 44.4 mol% $SiO_2$ (CAS glass). In the synthesis, all reagents were melted at 1500 °C for 1 h and rapidly quenched. This process was repeated several times to achieve homogeneity of chemical compositions.

### 2.2. NMR experiments

All NMR spectra were acquired at ambient temperature of 25 °C and spinning rate of 20 kHz, using a JEOL ECA-700 spectrometer equipped to a 16.4 T (Larmor frequency for $^{27}Al$ of 182.3 MHz) narrow bore magnet. A MAS controller allowed a sample rotor to spin at the accurate frequency of 20 ± 0.003 kHz. A home-built NMR probe generates r.f. field strengths up to 96 kHz that was evaluated from the 90° pulse length for 1.0 M $AlCl_3$ aqueous solution. Chemical shift scale in ppm was referenced to 1.0 M $AlCl_3$ aqueous solution (−0.1 ppm). After a bottom part of a 3.2 mm zirconia ($ZrO_2$) sample rotor was filled with $Na_2SO_4$ for magic angle adjustment, the center part was filled with kaolin or glass.

We have decided that precise adjustment of magic angle was achieved when single resonance was observed in a $^{23}Na$ STMAS spectrum of $Na_2SO_4$ that has one crystallographically distinct Na site. In the preliminary examination, the magic angle once adjusted can be kept at least for 2 weeks without miss setting more than 0.002°, unless the probe was detached from a superconducting magnet. Actually, a $^{23}Na$ STMAS spectrum was acquired after the STMAS experiments to confirm the perfect setting of magic angle.

Several *z*-filter type STMAS and MQMAS pulse sequences (Fig. 1) were used for the comparison of sensitivity and resolution. Sign discrimination of signals in the experiments was achieved by hyper-complex (states) method. The $F_1$ spectral width is matched to the spinning rate so that the $t_1$ increment is equal to the MAS rotor period (=a reciprocal of rotor frequency). In the STMAS experiments, the undesired signals arising from CT–CT auto correlation and outer satellite transitions are eliminated by inserting a selective soft π pulse at the beginning (DQ) or at the end (DQF) of the $t_1$ duration (Fig. 1a–c). The final π/2 soft pulse was applied using 10% of the r.f. field strength for hard pulses. Furthermore, SPAM technique is implemented into DQF-STMAS and 3Q-zfilter pulse sequence to improve the sensitivity. In the SPAM experiments, the echo and antiecho signals were collected separately and added to construct a FID for data processing, because it is impossible to acquire the echo and antiecho simultaneously.

To compare sensitivity, STMAS and MQMAS spectra were obtained with the same total scan time and the same points in $F_1$ and $F_2$ dimensions. The total acquisition of each experiment was completed in 2 h 8 min for kaolin and 3 h 25 min for glass.

The pulse lengths in each pulse sequence were optimized so that the Fourier transform of ST–CT correlation signal is maximized. The typical pulse lengths optimized for the case using maximum r.f. field strength are summarized in Table 1. The resultant MQMAS and STMAS spectra are expressed with the unified ppm scaling [16] where the resonance is located in the same place whatever coherence order is used.

## 3. Results

### 3.1. Comparison of MQMAS and STMAS spectra

The representative STMAS and 3QMAS spectra for kaolin and glass are shown in Fig. 2. $F_1$ projection provides the spectrum without effects of the second-order quadrupolar interaction, while $F_2$ projection provides one corresponding to a conventional MAS spectrum that still contains the second-order quadrupolar interaction. In the representative STMAS and 3QMAS NMR spectra for kaolin (Fig. 2a and b), a 6-coordinated Al site ($^{[6]}Al$) is observed, while in those for glass (Fig. 2c and d), a main 4-coordinated Al site ($^{[4]}Al$) was observed in down field region and a minor 5-coordinated Al site ($^{[5]}Al$) was observed in upper field one. The comparison of sensitivity and resolution described below was concerned with the $^{[6]}Al$ site of kaolin and the $^{[4]}Al$ one of glass.

As seen from Fig. 2, main characteristics in STMAS spectra are consistent with those in 3QMAS spectra of the corresponding sample. The broadening along CS and QIS lines in the spectra means the distribution of chemical shifts and that of quadrupolar interactions, respectively. The large distribution in chemical shift and quadurpolar interaction is found for the glass. In addition, tails to lower

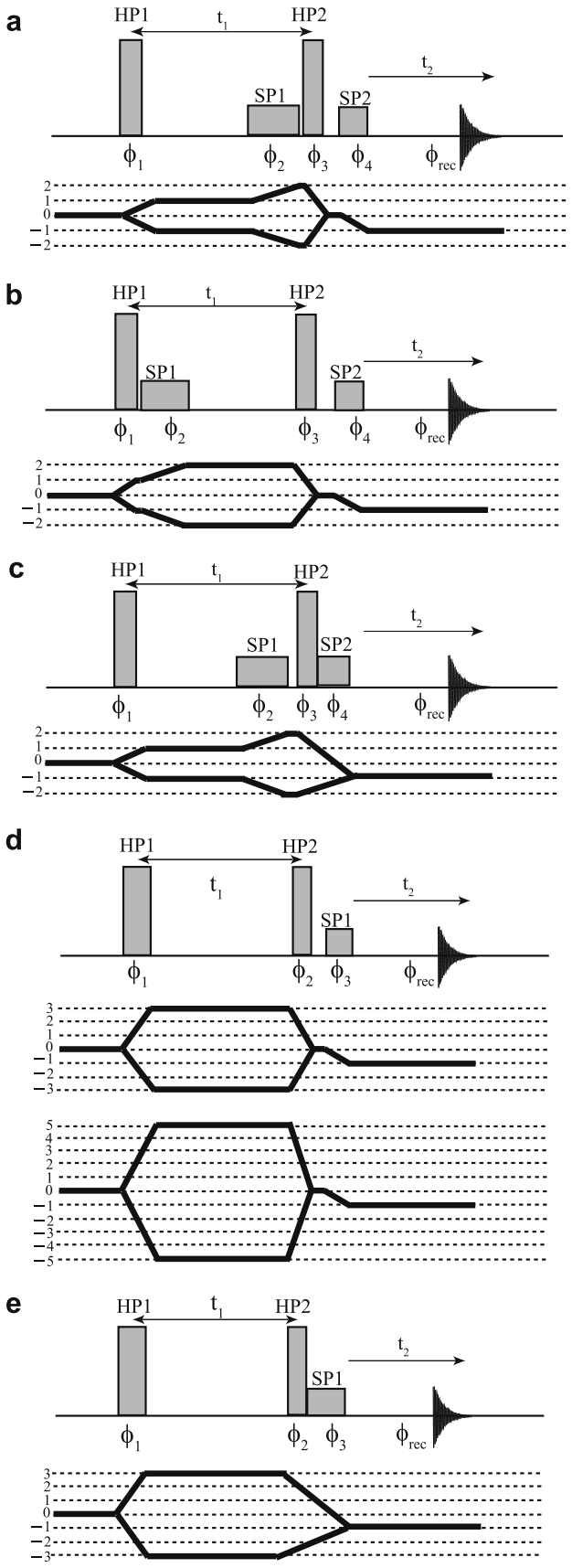


**Fig. 1.** STMAS (a–c) and MQMAS (d, e) pulse sequences used in this study and their coherence transfer pathways. (a) DQF, (b) DQ, (c) DQF-SPAM, (d) 3Qz & 5Qz, (e) 3Q-SPAM. Phase cycles ($\varphi_n$: $n$ = 1, 2, 3,...) are listed in Appendix.

frequency on $F_2$ projections of STMAS and MQMAS spectra are recognized in both samples. This is a typical feature observed in MAS spectra of other disordered materials [1].

The isotropic chemical shifts ($\delta_{iso}$) and quadrupolar products ($P_Q$) were estimated from the following equations [18]:

$$\delta_{iso} = \frac{17}{27}\delta_{F1} + \frac{10}{27}\delta_{F2}$$

$$P_Q = \sqrt{\frac{170}{80}\frac{(4S(2S-1))^2}{(4S(4S+1)-3)}(\delta_{F1}-\delta_{F2})\frac{\nu_0^3}{10}}$$

where $S$ is the spin quantum number, and $\nu_0$ is the Larmor frequency for $^{27}$Al. $\delta_{F1}$ and $\delta_{F2}$ are the positions (in ppm) of center of gravity for the Al peak on $F_1$ and $F_2$ projections, respectively.

These values are identical whichever STMAS and MQMAS spectra were selected, and found to be $\delta_{iso}$ = 8.9 ± 0.3 ppm and $P_Q$ = 3.5 ± 0.3 MHz for $^{[6]}$Al site of kaolin, and $\delta_{iso}$ = 71.5 ± 0.5 ppm and $P_Q$ = 6.8 ± 0.6 MHz for $^{[4]}$Al site of glass. These values are reasonably consistent with those of the previous studies [16,17,19]. However, it should be noted that the $P_Q$ estimated for glass is just an average value of widely-distributed quadrupolar interaction. According to the extraction method proposed by Goldbourt et al. [20], it is found that the $P_Q$ of glass actually ranges from 0.3 to 10.4 MHz.

### 3.2. Comparison of sensitivity

Typical $F_2$ projections of STMAS and MQMAS spectra for kaolin and glass (Fig. 3) demonstrate that STMAS pulse sequences exhibit higher sensitivity than 3QMAS ones. Quantitative comparison of sensitivity has been performed using S/N ratios for the equal amounts of powder samples.

The change of S/N ratios depending on applied r.f. field strengths (Fig. 4) shows that sensitivity of both STMAS and MQMAS heightens with increasing the strength of r.f. field. This result indicates that high r.f. field strengths are essential to get higher sensitivity in STMAS and MQMAS experiments [6,21]. Furthermore, high sensitivity is obtained in the following order of pulse sequences: DQF-SPAM, DQF, DQ, 3Q-SPAM, and 3Qz. For kaolin, DQF-SPAM shows 4.5 times higher sensitivity than 3Qz. This means that DQF-SPAM needs only one day to obtain a high-resolution spectrum that is collected by 3Qz in 20 days. Even if sensitivity of 3QMAS is improved by implementing SPAM technique (3Q-SPAM), its sensitivity is less than that of any STMAS pulse sequence. Such a sensitivity advantage of STMAS over MQMAS is partly ascribed to the effect of spinning rate on sensitivity: as a spinning rate increases, sensitivity of MQMAS reduces remarkably, while that of STMAS is kept almost constant [6].

Sensitivity advantage of STMAS over MQMAS is quantitatively different between kaolin and glass. For glass, smaller degree of sensitivity enhancement was obtained by STMAS. This well agrees with Ashbrook and Wimperis [6], who also stated that sensitivity advantage of STMAS changes depending on samples. This might be due to the difference in strength of quadrupolar interaction, or to the difference in crystallinity i.e. distribution of chemical shifts and quadrupolar interaction.

### 3.3. Comparison of resolution

To compare the resolution, the full widths at half maximum (FWHM) were estimated from the $F_1$ projections (Fig. 5). Because the FWHMs are independent of the applied r.f. field strengths, the FWHM obtained at maximum r.f. field strength was selected as a typical one. For easy comparison, the FWHM normalized by that of 3Qz was listed in Table 2.

**Table 1**
Optimized pulse lengths (μs) when the maximum r.f. field strength of 96 kHz was applied for hard pulses (HP1, HP2).

| | | DQF-SPAM | DQF | DQ | 3Q-SPAM | 3Qz |
|---|---|---|---|---|---|---|
| Kaolin | HP1 | 1.5 | 1.3 | 1.4 | 2.8 | 3 |
| | HP2 | 0.6 | 0.8 | 0.8 | 0.8 | 1 |
| | SP1 | 20 | 20 | 20 | 15 | 15 |
| | SP2 | 10 | 10 | 10 | – | – |
| Glass | HP1 | 1.2 | 1.2 | 1 | 2.4 | 2.4 |
| | HP2 | 0.8 | 0.8 | 0.8 | 0.6 | 1 |
| | SP1 | 20 | 20 | 20 | 15 | 15 |
| | SP2 | 10 | 10 | 10 | – | – |

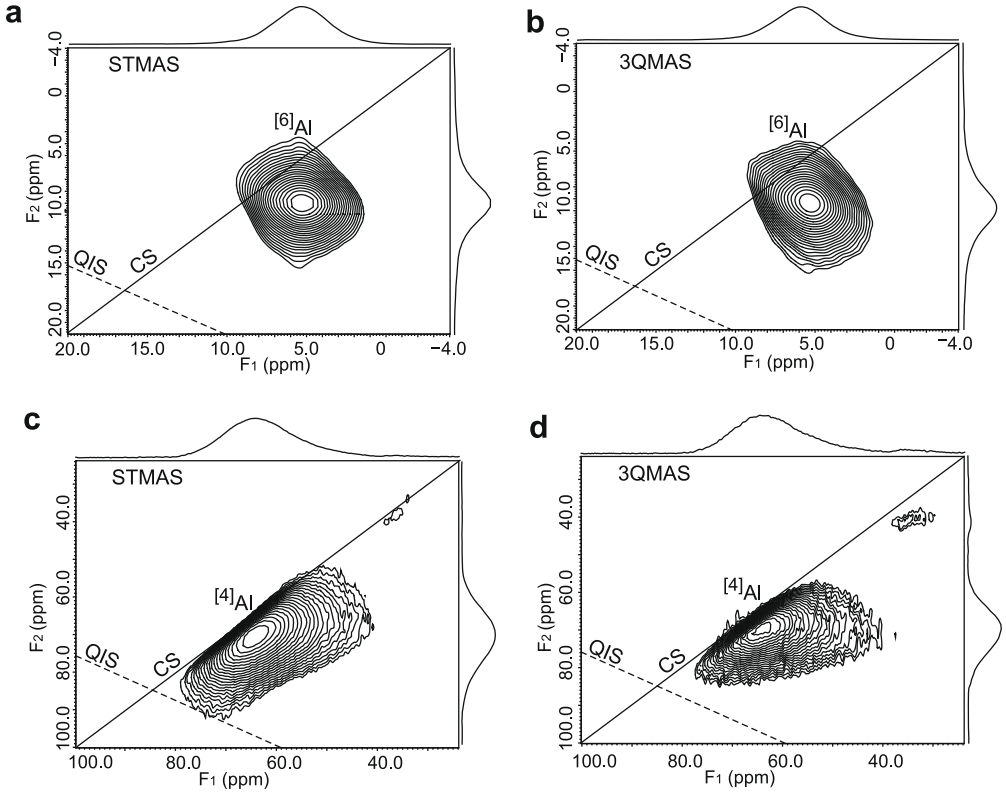


**Fig. 2.** $^{27}$Al STMAS and 3QMAS spectra of kaolin and glass. The STMAS spectra shown were obtained with DQF pulse sequence, whereas 3QMAS spectra were obtained with 3Qz one. DQF-STMAS (a) and 3QMAS (b) spectra of kaolin were recorded with a recycle delay of 2.5 s by averaging 48 transients with 32 $t_1$ increments of 50 μs. DQF-STMAS (c) and 3QMAS (d) spectra of glass were recorded with a recycle delay of 4 s by averaging 48 transients with 32 $t_1$ increments of 50 μs. A solid line indicates the chemical shift (CS) axis, while a dotted line indicates the quadrupolar induced shift (QIS).

As seen from Table 2, the highest resolution for kaolin is obtained by 5Qz. DQF, DQF-SPAM, 3Qz, and 3Q-SPAM provide the second highest resolution, whereas DQ possesses the lowest resolution. These results for kaolin are qualitatively consistent with the relationship of homogeneous broadening factors for $I = 5/2$ nuclei reported by Trebosc et al. [10]. Furthermore, it is clearly shown that implementation of SPAM technique has no effect on line widths to show the comparable resolution with that of the original *z*-filter experiments. In the case of kaolin, the $^1$H–$^{27}$Al heteronuclear dipolar coupling has been considered to be very small, because line widths and line shapes are consistent in $^{27}$Al MAS spectra with and without $^1$H decoupling. However, the dephasing caused by $^1$H–$^{27}$Al heteronuclear dipolar coupling is actually proportional to the selected quantum level [22]. Thus, if the $^1$H–$^{27}$Al coupling remains residual under such a fast spinning of 20 kHz, the resolution of MQMAS spectra may be slightly improved by the application of decoupling with a relatively high r.f. field. In particular, the resolution of 5Qz might be more improved. Hence, as a result of $^1$H decoupling, the relative line widths of 5Qz (Table 2) might be close to the reported one [10], although the qualitative relationship of resolution listed in Table 2 would not be changed.

For glass, 5QMAS possesses the highest resolution as well as for kaolin. However, relationship of FWHM in STMAS and 3QMAS is not consistent with a simulated result [10]. Any STMAS pulse sequence shows lower resolution than 3Qz and 3Q-SPAM. Furthermore, DQF and DQ show almost the same resolution. The lower resolution in STMAS is often ascribed to miss setting of magic angle [10,18]. However, it is impossible in the present study to suppose the situation where the miss setting occurred only for glass. Therefore, this result suggests that STMAS spectra of glass might be broadened by other factors.

## 4. Discussion

### 4.1. Resolution for inorganic materials with practical importance

Isotropic STMAS spectra of glass have slightly wider line widths than MQMAS ones. Actually, this result can be interpreted in two

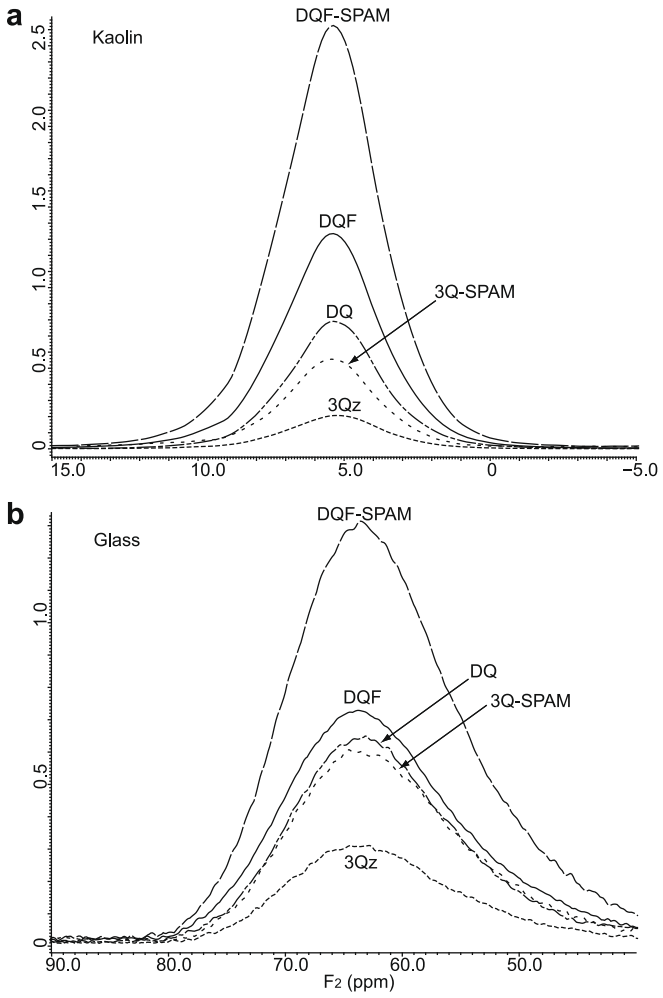


**Fig. 3.** Stack plots of $F_2$ projections for kaolin (a) and glass (b). These spectra were extracted from the $^{27}$Al STMAS and 3QMAS spectra obtained at the maximum r.f. field strength of 97 kHz.

ways; as first way, the resolution of STMAS is certainly reduced in the case of glass by a factor that affects on only STMAS experiments.

The broadening in STMAS spectra is sometimes ascribed to insufficient setting of magic angle or to instability of MAS speed [10,18]. In this study, these factors, however, cannot be a primary reason to generate the additional broadening for glass, because the perfect setting of magic angle and the stable spinning (20 ± 0.003 kHz) are guaranteed by the preliminary examinations. In fact, the reasonable result is obtained for the resolution of kaolin.

Higher-order interactions are considered to be possible mechanisms. Third-order quadrupolar interaction is first possibility to produce the broadening. This interaction affects neither central transitions, nor symmetrical multi quantum ones [24]. Effects of this higher order interaction can be observed when the strong quadrupolar interaction is present [25,26]. The third order effect is proportional to $(\nu_q^3/\nu_0^2)$, where $\nu_q$ is quadrupolar frequency, $\nu_0$ Larmor frequency [26]. Gan et al. [25] has stated that at a magnetic field of 11.7 T, the third-order quadrupolar interaction broadens the STMAS spectra for Al site in andalusite with lager $C_q$ of 15.3 MHz ($\nu_q = 15.3/2\pi = 2.3$ MHz, $\nu_q^3/\nu_0^2 = 7.2 \times 10^{-4}$), but not for the other one with smaller $C_q$ of 5.6 MHz ($\nu_q = 5.6/2\pi = 0.8$ MHz, $\nu_q^3/\nu_0^2 = 4.2 \times 10^{-5}$) when magic angle missset is quite small (<0.001°). In this study using a higher magnetic field of 16.4 T, the value of $\nu_q^3/\nu_0^2$ is calculated to be $5.7 \times 10^{-6}$ for the $^{[6]}$Al site in kaolin, and $4.5 \times 10^{-5}$ for the $^{[4]}$Al site in glass, respectively. These values are almost the same or less than that for the smaller $C_q$ site in andalusite [25], indicating that effects of third order quadrupolar interaction are extremely small. Therefore, at least in this study, the third order quadrupolar interaction cannot cause the additional broadening in the STMAS spectra of glass.

Second-order quadrupolar–dipolar cross-term interaction between quadrupolar nuclei and $I = 1/2$ nuclei is second possibility. As well as third-order quadrupolar interaction, this cross-term interaction does not affect symmetrical transitions [27]. Al and Si atoms in glass exist as tetrahedral oxide species. This means that Si and Al atoms are separated each other via bridging oxygen atoms. Furthermore, in addition to low natural abundance of $^{29}$Si (4.7%), the dipole moment of $^{29}$Si is originally small. Therefore, Si and Al atoms are too far away to yield quadrupolar–dipolar interaction between them. The second-order quadrupolar–dipolar interaction between Al and the adjacent atoms, O, are also quite small, because of the extremely low natural abundance of $^{17}$O (0.038%) and its small dipole moments. Second-order quadrupolar–dipolar cross-term interactions, hence, should not be a reason for additional broadening on the STMAS spectra of glass.

Second-order quadrupolar–chemical shift anisotropy (CSA) cross-term interaction is third possibility. As well as the above higher-order interactions, the quadrupolar–CSA cross-term interaction

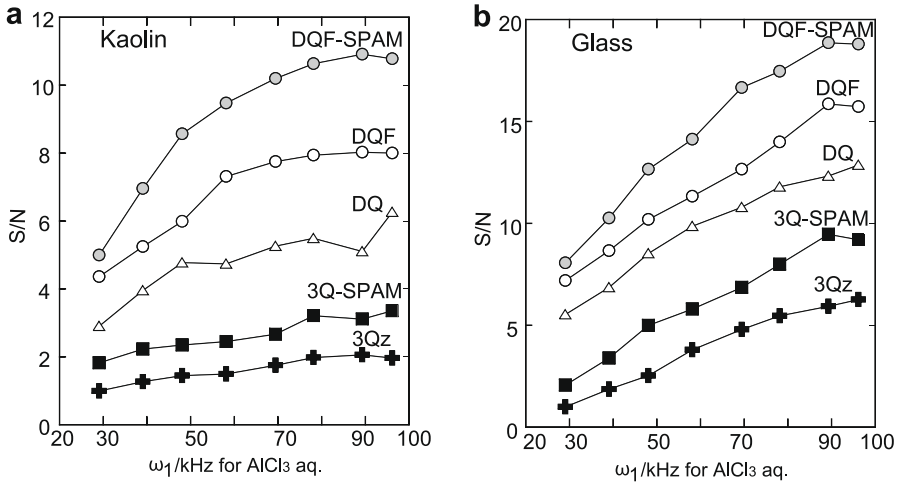


**Fig. 4.** Variation of signal to noise (S/N) ratios as a function of r.f. field strengths. Left side (a) is for kaolin and right side (b) is for glass. Note that the r.f. field strengths were determined from 90° pulse lengths for $AlCl_3$ aqueous solution.

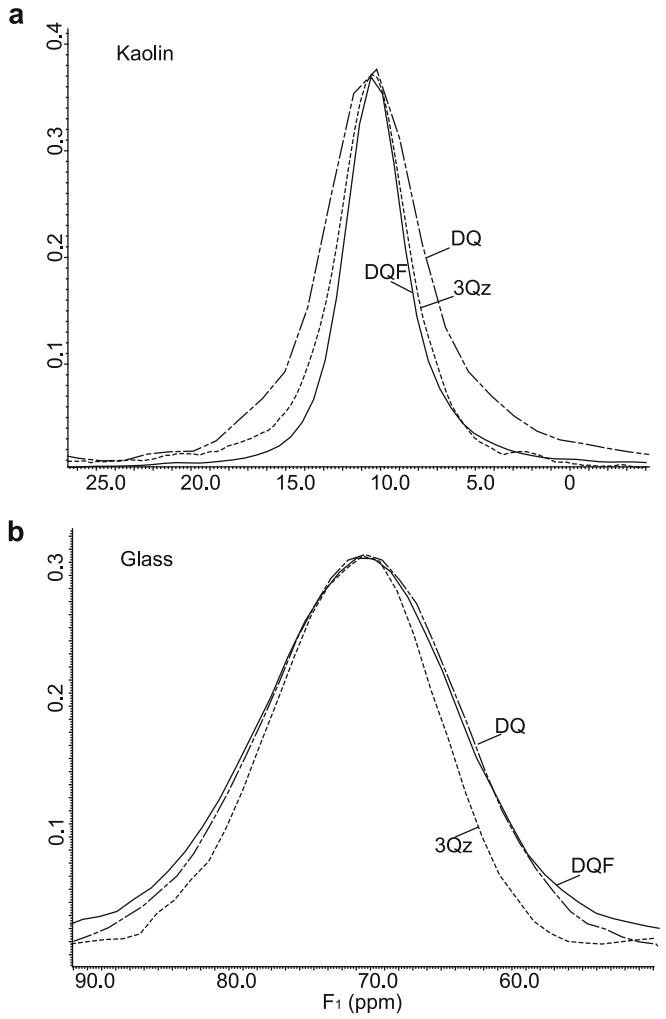


**Fig. 5.** Stack plots of $F_1$ projections for kaolin (a) and glass (b). A few selected projections of DQF, DQ, and 3Qz are shown. Note that peak top of all projections is made to have the same height for comparison of line widths.

**Table 2**
Comparison of resolution between STMAS and MQMAS experiments for $^{27}$Al ($I = 5/2$).

| | DQF-STMAS | DQF | DQ | 3Q-SPAM | 3Qz | 5Qz |
|---|---|---|---|---|---|---|
| Kaolin[a] | 0.96 | 0.96 | 1.31 | 0.90 | 1.00 | 0.45 |
| Glass[a] | 1.26 | 1.24 | 1.36 | 1.08 | 1.00 | 0.79 |
| Ref. values[b] | 1.00 | 1.00 | 1.77 | 1.00 | 1.00 | 0.24 |

The same broadening factors are assumed for 3Qz and 3Q-SPAM sequences.
[a] The FWHM of each pulse sequence is normalized by that of *z*-filter 3QMAS sequence (3Qz).
[b] Homogeneus broadening factors reported by Trebosc et al. [10].

does not affect central transition nor symmetrical multiple quantum ones. When CSA anisotropy is sufficiently large, the broadening or splitting induced by the cross-term interaction is recognized in STMAS spectra [28]. On the contrary to third-order quadrupolar interaction, second-order CSA–quadrupolar cross-term interaction is independent of the strength of static magnetic field [26]. Thus, effects of the quadrupolar–CSA cross-term interaction might be left even under high magnetic fields. However, the CSA of glass is rather small in magnitude, although the chemical shifts has large distribution, because of its structural disorder. As a consequence, any higher-order interaction examined here cannot be a fundamental mechanism to explain the broadening in STMAS spectra.

A well-known broadening in STMAS spectra has been reported as motional broadening [23]. This phenomenon is theoretically treated as the result of molecular reorientation under MAS. In fact, motional broadening is observed on STMAS spectra of hydroxyl chondrodite and hydroxyl-clinohumite [24], where the rotational motion of $^1$H atoms has been considered to generate the modulation of local field. In the case of glasses, the motional broadening is not caused in the same manner because of the absence of structural OH groups. However, it might be caused by framework flexibility in the structure of glass.

As second interpretation of the wider line widths, STMAS provides more appropriate spectra where a large distribution of chemical shifts more faithfully appears than in the 3QMAS spectra. Thus, STMAS may become more useful in structural analysis of disordered materials.

In any case, such a difference in line widths of glass is too small to be considered as inferior resolution of STMAS. On the contrary, we have considered that STMAS can possess resolution that is comparable to 3QMAS in the structural analysis of crystalline and non-crystalline materials.

### *4.2. Optimum r.f. field strength and total estimation of sensitivity advantage of STMAS*

As seen from Fig. 4, S/N ratios of STMAS and 3QMAS grow with increasing the strength of r.f. field. This result means that at least in the r.f. field region used, high r.f. field strength is essential to gain a better S/N ratio. Based on the simulations to investigate ST and CT coherence amplitudes upon the flip angle for the spin $I = 3/2$ and 5/2, Ashbrook and Wimperis also demonstrated that a high r.f. field strength is advantageous to achieve high sensitivity [4]. This study experimentally confirmed that high r.f. field is necessary to get a good S/N ratio in STMAS and MQMAS experiments. However, one should be reminded that the optimum condition in STMAS and MQMAS are changed depending on the ratio of quadrupolar frequency ($\nu_Q$) to the r.f. field strength ($\nu_{r.f.}$). Thus, a high r.f. field strength is not always desirable for good sensitivity. In fact, using higher r.f. field strengths in MQMAS experiments sometimes lowers their sensitivity [20,29]. Therefore, when $\nu_Q$ of kaolin or glass, and $\nu_{r.f}$ in the present study are considered, we can conclude that high r.f. fields are beneficial for getting good S/N ratios.

STMAS certainly exhibits sensitivity advantage for a material with large quadrupolar interaction such as glass. However, for the glass, the degree of sensitivity enhancement obtained by STMAS clearly decreases compared to kaolin. Glass differs from kaolin as follows; its wider distribution in quadrupolar interaction, and more flexibility in structural framework. Hence, considering these points, we have examined a reason for the reduction.

The first consideration is given based on the distribution of quadrupolar interaction. In STMAS experiments, the rotational echoes are acquired under rotor-synchronized conditions. A basic pulse sequence of STMAS consists of two hard pulses which excite ST and correlate it to CT, respectively. Excitation and conversion of single-quantum coherence such as ST can be generated efficiently even under fast spinning condition. It is worth describing that their amplitudes actually depend on the strength of quadrupolar interaction. Ashbrook and Wimperis have indicated that maximum amplitudes of ST and CT coherences produced by excitation and conversion pulses, respectively, decrease as the strength of quadrupolar interaction increases [6]. This leads to lower S/N ratios recorded in STMAS experiments. In particular, the amplitudes of excitation and conversion of MQ coherences more rapidly decrease with increasing the strength of quadrupoalr interaction [29]. Therefore, the difference of sensitivity between STMAS and MQMAS should be smaller with decreasing the strength of quadrupolar interaction,

while the difference should be expanded with increasing its strength. Because the glass has a wide range in $P_Q$ ($0.3 \sim 10.3$ MHz), the sensitivity enhancement might be reduced for sites with smaller $P_Q$. As a result, compared to a material with the same $P_Q$ but with less distribution, the total sensitivity enhancement is also decreased by the contribution of smaller $P_Q$ sites. Hence, the largely distributed quadrupolar interaction in glass may cause the smaller magnitude of sensitivity enhancement.

Motional broadening in STMAS spectra might be also a reason for the reduction. This phenomenon recognized as a remarkable reduction of S/N ratios has been often observed in STMAS spectra of materials containing structural OH groups [23]. However, motional broadening is actually not limited to OH-bearing systems, but might be caused by framework flexibility of an amorphous material such as glass. In such a case, the total S/N ratios obtained by SMTAS should be also reduced, because of weak intensity of rotational echoes.

Nevertheless, it is worth noting again that all STMAS pulse sequences shows higher S/N ratios than 3QMAS ones. Therefore, we can conclude that STMAS applied to crystalline and non-crystalline materials as a whole exhibits higher sensitivity than MQMAS.

## 5. Conclusions

Through comparison of sensitivity and resolution between STMAS and MQMAS for $^{27}$Al of kaolin and glass, it is found that STMAS and 3QMAS exhibit a comparable resolution for both crystalline and non-crystalline materials. In any STMAS and MQMAS pulse sequences, the application of high r.f. fields is favored to get a better S/N ratio. At the maximum r.f. field strength, the sensitivity of STMAS is entirely higher than MQMAS that is combined with a signal enhancement scheme of SPAM. The degree of sensitivity enhancement obtained by STMAS may change depending on the distribution of quadrupolar interaction or on framework flexibility of the sample. Among the STMAS pulse sequences examined, DQF-SPAM is recommended for the local environment analysis of minor nuclei with spin I=5/2, which cannot be accomplished by conventional MQMAS.

## Acknowledgment

The authors thank two anonymous reviewers for their constructive comments.

## Appendix A

Table A1. Phase cycling for the STMAS pulse sequences (spin I = 5/2) shown in Fig. 1(a–c).

| | |
|---|---|
| | *DQF- and DQ-STMAS* |
| $\phi1$ | {0} |
| $\phi2$ | {2(0), 2(180)} |
| $\phi3$ | {4(0), 4(90), 4(180), 4(270)} |
| $\phi4$ | {0} |
| $\phi$rec | {0, 180, 180, 0, 180, 0, 0, 180} |
| | *DQF-SPAM STMAS* |
| $\phi1$ | {0, 180, 90, 270} |
| $\phi2$ | {4(0), 4(270), 4(180), 4(90)} |
| $\phi3$ | {0} |
| $\phi4$ | {(0), (180)} |
| $\phi$rec | {(0, 90, 180, 270, 90, 180, 270, 0, 180, 270, 0, 90, 270, 0, 90, 180), (180, 90, 0, 270, 90, 0, 270, 180, 0, 270, 280, 90, 270, 180, 90, 0)} |

Table A2. Phase cycling for the MQMAS pulse sequences (spin I = 5/2) shown in Fig. 1(d) and (e).

| | |
|---|---|
| | *3QMAS with z-filter (24 cycles)* |
| $\phi1$ | {0, 60, 120, 180, 240, 300} |
| $\phi2$ | {0} |
| $\phi3$ | {3(0, 180), 3(180, 0), 3(90, 270), 3(270, 90)} |
| $\phi$rec | {6(0), 6(180), 6(90), 6(270)} |
| | *5QMAS with-z-filter (40 cycles)* |
| $\phi1$ | {0, 36, 72, 108, 144, 180, 216, 252, 288, 324} |
| $\phi2$ | {0} |
| $\phi3$ | {5(0, 180), 5(180, 0), 5(90, 270), 5(270, 90)} |
| $\phi$rec | {10(0), 10(180), 10(90), 10(270)} |
| | *3QMAS with SPAM (24 cycles)* |
| $\phi1$ | {0, 30, 60, 90, 120, 150, 180, 210, 240, 270, 300, 330} |
| $\phi2$ | {0} |
| $\phi3$ | {12(0), 12(180)} |
| $\phi$rec | {3(0, 270, 180, 90), 3(0,90, 180, 270)} |

## References

[1] A.P.M. Kentgens, A practical guide to solid state NMR of half-inter quadrupolar nuclei, Geoderma 80 (1997) 271–306.
[2] K. Ueda, Y. Onuki, Physics of heavy electron systems, Shokabo, Tokyo, 1998, pp. 110–112.
[3] A. Llor, J. Virlet, Towards high-resolution NMR of more nuclei in solids: sample spinning with time-dependent spinner axis angle, Chem. Phys. Lett. 152 (1988) 248–253.
[4] L. Frydman, J.S. Harwood, Isotropic spectra of half-integer quadrupolar spins from bidimensional magic-angle spinning NMR, J. Am. Chem. Soc. 117 (1995) 5367–5368.
[5] Z. Gan, Isotropic NMR spectra of half-integar quadrupolar nuclei using satellite transitions and magic-angle-spinning, J. Am. Chem. Soc. 122 (2000) 3242–3243.
[6] S.E. Ashbrook, S. Wimperis, High-resolution NMR of quadrupolar nuclei in solids: the satellite-transition magic angle spinning (STMAS) experiment, Prog. Nucl. Magn. Reson. Spectrosc. 45 (2004) 53–108.
[7] S.E. Ashbrook, S. Wimperis, Satellite-transition MAS NMR of Spin $I = 3/2$, 5/2, 7/2, and 9/2 nuclei: sensitivity, resolution, and practical implementation, J. Magn. Reson. 156 (2002) 269–281.
[8] K.J. Pike, S.E. Ashbrook, S. Wimperis, Two dimensional satellite-transition MAS NMR of quadrupolar nuclei: shifted echoes, high-spin nuclei and resolution, Chem. Phys. Lett. 345 (2001) 400–408.
[9] N.G. Dowell, S.E. Ashbrook, S. Wimperis, Satellite-transition MAS NMR of low-$\gamma$ nuclei at natural abundance: sensitivity, practical implementation, and application to$^{39}$K ($I = 3/2$) and $^{25}$Mg ($I = 5/2$), J. Phys. Chem. B 108 (2004) 13292–13299.
[10] J. Trebosc, J.P. Amoureux, Z. Gan, Comparison of high-resolution solid-state NMR MQMAS and STMAS methods for half-integer quadrupolar nuclei, Solid State Nucl. Magn. Reson. 31 (2007) 1–9.
[11] C. Huguenard, F. Taulelle, B. Knott, Z. Gan, Optimizing STMAS, J. Magn. Reson. 156 (2004) 131–137.
[12] H.T. Kwak, Z. Gan, Double-quantum filtered STMAS, J. Magn. Reson. 164 (2003) 369–372.
[13] Z. Gan, H.T. Kwak, Enhancing MQMAS sensitivity using signals from coherence transfer pathways, J. Magn. Reson. 168 (2004) 346–351.
[14] T.J. Ball, S. Wimperis, Use of SPAM and FAM pulses in high-resolution MAS NMR spectroscopy of quadrupolar nuclei, J. Magn. Reson. 187 (2007) 343–351.
[15] J.P. Amoureux, L. Delevoye, G. Fink, F. Taulelle, A. Flambard, L. Montagne, Implementing SPAM into STMAS: a net sensitivity improvement in high-resolution NMR of quadrupolar nuclei, J. Magn. Reson. 175 (2005) 285–299.
[16] K.J. Pike, R.P. Malde, S.E. Ashbrook, J. McManus, S. Wimperis, Multiple-quantum MAS NMR of quadrupolar nuclei. Do five-, seven- and nine-quantum experiments yield higher resolution than the three quantum experiment?, Solid State Nucl Magn. Reson. 16 (2000) 203–215.
[17] K. Kanehashi, J.F. Stebbins, In situ high temperature 27Al NMR study of structure and dynamics in a calcium aluminosilicate glass and melt, J. Non-Cryst. Solids 353 (2007) 4001–4010.
[18] J.-P. Amoureux, C. Huguenard, F. Engelke, F. Taulelle, Unified representation of MQMAS and STMAS NMR of half inter quadrupolar nuclei, Chem. Phys. Lett. 356 (2002) 497–504.
[19] K. Kanehashi, K. Saito, First application of 27Al multiple quantum magic-angle spinning nuclear magnetic resonance at 16.4 T to inorganic matter in natural coals, Energy Fuels 18 (2004) 1732–1737.
[20] A. Goldbourt, M.V. Landau, S. Vega, Characterization of aluminum species in alumina multilayer grafted MCM-41 using $^{27}$Al FAM(II)-MQMAS NMR, J. Phys. Chem. B 107 (2003) 724–731.

[21] J. Kanellopoulos, D. Freude, A. Kentgens, A practical comparison of MQMAS techniques, Solid State Nucl. Magn. Reson. 32 (2007) 99–108.
[22] S. Ganapathy, L. Delevoye, J.P. Amoureux, P.K. Madhu, Heteronuclear dipolar decoupling effects on multiple-quantum and satellite-transition magic angle spinning NMR spectra, Magn. Reson. Chem. 46 (2008) 948–954.
[23] S.E. Ashbrook, S. Antonijevic, A.J. Berry, S. Wimperis, Motional broadening: an important distinction between multiple-quantum and satellite-transition MAS NMR of quadrupolar nuclei, Chem. Phys. Lett. 364 (2002) 634–642.
[24] A.D. Bain, Simple proof that third-order quadrupole perturbations of the NMR central transitions of half-integral nuclei are zero, J. Magn. Reson. 179 (2006) 308–310.
[25] Z. Gan, P. Srinivasan, J.R. Quine, S. Steuernagel, B. Knott, Chem. Phys. Lett. 367 (2003) 163.
[26] S. Wi, S.E. Ashbrook, S. Wimperis, Second-order quadrupole-shielding effects in magic angle spinning solid-state nuclear magnetic resonance, J. Chem. Phys. 118 (2003) 3131–3140.
[27] G. Wu, The influence of the heteronuclear dipolar interaction on nuclear magnetic resonance spectra of quadrupolar nuclei, Mol. Phys. 95 (1998) 1177–1183.
[28] S. Wi, L. Frydman, Quadrupolar-shielding cross relations in solid state nuclear magnetic resonance: detecting antisymmetric components in chemical shift tensors, J. Chem. Phys. 116 (2002) 1551–1561.
[29] J.P. Amoureux, C. Fernandez, Triple quintuple and higher order multiple quantum MAS NMR of quadrupolar nuclei, Solid State Nucl. Magn. Reson. 10 (1998) 212–213.